JOURNAL OF BACTERIOLOGY, July 2001, p. 4061–4070 Vol. 183, No. 13
0021-9193/01/$04.00+0 DOI: 10.1128/JB.183.13.4061–4070.2001

Microbial Origin of Plant-Type 2-Keto-3-Deoxy-D-*arabino*-Heptulosonate 7-Phosphate Synthases, Exemplified by the Chorismate- and Tryptophan-Regulated Enzyme from *Xanthomonas campestris*

GUILLERMO GOSSET,[1]* CAROL A. BONNER,[2] AND ROY A. JENSEN[2,3,4]

Departamento de Microbiología Molecular, Instituto de Biotecnología, Universidad Nacional Autónoma de México, Cuernavaca, Morelos 62250, Mexico[1]; Department of Microbiology and Cell Science, University of Florida, Gainesville, Florida 32611[2]; Department of Chemistry, City College of New York, New York, New York 10031[3]; and BioScience Division, Los Alamos National Laboratory, Los Alamos, New Mexico 87544[4]

Received 31 October 2000/Accepted 3 April 2001

Enzymes performing the initial reaction of aromatic amino acid biosynthesis, 2-keto-3-deoxy-D-*arabino*-heptulosonate 7-phosphate (DAHP) synthases, exist as two distinct homology classes. The three classic *Escherichia coli* paralogs are $AroA_I$ proteins, but many members of the *Bacteria* possess the $AroA_{II}$ class of enzyme, sometimes in combination with $AroA_I$ proteins. $AroA_{II}$ DAHP synthases until now have been shown to be specifically dedicated to secondary metabolism (e.g., formation of ansamycin antibiotics or phenazine pigment). In contrast, here we show that the *Xanthomonas campestris* $AroA_{II}$ protein functions as the sole DAHP synthase supporting aromatic amino acid biosynthesis. *X. campestris* $AroA_{II}$ was cloned in *E. coli* by functional complementation, and genes corresponding to two possible translation starts were expressed. We developed a 1-day partial purification method (>99%) for the unstable protein. The recombinant $AroA_{II}$ protein was found to be subject to an allosteric pattern of sequential feedback inhibition in which chorismate is the prime allosteric effector. L-Tryptophan was found to be a minor feedback inhibitor. An N-terminal region of 111 amino acids may be located in the periplasm since a probable inner membrane-spanning region is predicted. Unlike chloroplast-localized $AroA_{II}$ of higher plants, *X. campestris* $AroA_{II}$ was not hysteretically activated by dithiols. Compared to plant $AroA_{II}$ proteins, differences in divalent metal activation were also observed. Phylogenetic tree analysis shows that $AroA_{II}$ originated within the *Bacteria* domain, and it seems probable that higher-plant plastids acquired $AroA_{II}$ from a gram-negative bacterium via endosymbiosis. The *X. campestris* $AroA_{II}$ protein is suggested to exemplify a case of analog displacement whereby an ancestral $aroA_I$ species was discarded, with the $aroA_{II}$ replacement providing an alternative pattern of allosteric control. Three subgroups of $AroA_{II}$ proteins can be recognized: a large, central group containing the plant enzymes and that from *X. campestris*, one defined by a three-residue deletion near the conserved KPRS motif, and one possessing a larger deletion further downstream.

Microorganisms and plants engage 3-deoxy-D-*arabino*-heptulosonate 7-phosphate (DAHP) synthase (EC 4.1.2.15) as the initial catalyst for the commitment of phosphoenolpyruvate (PEP) and erythrose 4-phosphate (E4P) to the biosynthesis of aromatic amino acids, vitamin K, folic acid, and ubiquinone (4). The pathway contributes heavily to the biochemical individuality of organisms, with an enormous variety of peripheral branch connections known. Various pigments, siderophores, signaling compounds, defense metabolites, structural compounds, antibiotics, and other secondary metabolites are derived from this pathway (4).

DAHP synthases fall into two distinct homology families. The $AroA_I$ family is divided into subfamilies $AroA_{I\alpha}$ and $AroA_{I\beta}$ (32). The $AroA_{I\alpha}$ subfamily is widely represented in gram-negative bacteria in which differentially regulated paralogs are commonly expressed, as exemplified by *Escherichia coli* (three paralogs). DAHP synthase members of the $AroA_{I\beta}$ subfamily are more closely related to 3-deoxy-D-*manno*-octulosonate 8-phosphate synthases than to members of the $AroA_{I\alpha}$ subfamily of DAHP synthases (32).

The $AroA_{II}$ family of DAHP synthases was first identified in higher plants in which the member proteins are chloroplast localized (11), subject to sequential feedback inhibition by L-arogenate (8), and hysteretically activated by dithiothreitol (DTT) (7, 11). The eventual availability of sequence data for these plant-type DAHP synthases revealed that they comprise a separate homology group quite distinct from the $AroA_I$ family (4). Microbial $AroA_{II}$ DAHP synthases were later identified in *Neurospora crassa* and in several species of *Streptomyces* (34). Species of *Pseudomonas* that make phenazine pigments employ a pathway encoded by genes which include an $AroA_{II}$ type of DAHP synthase (21, 23). Other microbial $AroA_{II}$ proteins have a specialized role in antibiotic biosynthesis (3, 5, 17, 25, 30). Thus, the emerging perspective is that microbial $AroA_{II}$ enzymes generally participate in a mode of secondary metabolism in which various antibiotic agents are made. In this context two general roles for $AroA_{II}$ can be discerned as follows. (i) $AroA_{II}$ is necessary for a crucial catalytic step for the

* Corresponding author. Mailing address: Departamento de Microbiología Molecular, Instituto de Biotecnología, Universidad Nacional Autónoma de México, Apdo. Postal 510-3, Cuernavaca, Morelos 62250, Mexico. Phone: 52-73-291648. Fax: 52-73-172388. E-mail: gosset@ibt.unam.mx.

TABLE 1. Strains and plasmids

Strain or plasmid	Relevant characteristics	Source or reference
E. coli strains		
XL1 Blue MR	Δ(*mcrA*)*183* Δ(*mcrCB-hsdSMR-mrr*)*173 endA1 supE44 thi-1 recA1 gyrA96 relA1 lac*	Stratagene
AB3248	*aroF363 aroG365 aroH367 proA2 argE3 elv-7 his-4 lac gal-2 tsx-358 thi*	35
BL21(DE3)	F^- *ompT hsdS*$_B$ (r_B^- m_B^-) *gal dcm*; with DE3, a λ prophage carrying T_7 RNA polymerase	Novagen
DH5α	F^-e14^- (*mcrA*) *hsdR514* (r_K^- m_K^+) *recA1 endA1 gyrA96 thi-1 relA1 supE44*	Gibco-BRL
X. campestris strain		
ATCC 33436		20
Plasmids		
pTacIQ	ColE1 ori, *lacI*, *tac* promoter, Amp^r	Van Kimmenade
pTacIQ2.3	Derivative of pTacIQ containing a 6.5-kb fragment of *X. campestris* DNA	This work
pTacIQ2.3B	Derivative of pTacIQ containing a 2.7-kb fragment of *X. campestris* DNA	This work
pET-24b$^+$	Contains the T7/*lacO* promoter	Stratagene
pET-M1	Derivative of pET-24b$^+$ containing a PCR product encoding $AroA_{II}$ starting from the first putative translation start site	This work
pET-M2	Same as pET-M1 but containing a PCR product encoding $AroA_{II}$ starting from the second putative translation start site	This work

production of a molecule (e.g., 3-amino, 5-hydroxybenzoate) acting as a starter unit for polyketide assembly, as exemplified by organisms producing ansamycin antibiotics (3, 5, 18) or rapamycin (25). (ii) $AroA_{II}$ is important for generating precursors for anthranilate synthesis. Anthranilate is then incorporated into phenazine structures (21, 23) or into menaquinone-like structures which inhibit electron transport (30). The type-i $AroA_{II}$ proteins apparently possess an altered substrate specificity in which either an aminated derivative of E4P is recognized or an additional overall aminating capability exists (17), whereas type-ii $AroA_{II}$ proteins possess normal substrate specificity.

Most microbial $AroA_{II}$ proteins annotated in the National Center for Biotechnology Information's nonredundant and Finished and Unfinished Genomes databases were identified by sequence inference and by context of operon organization without any enzymological characterization, e.g., the phenazine pigment operons (21, 23). The most detailed characterization of $AroA_{II}$ DAHP synthases has been from *Streptomyces* and *Neurospora*, where sequence information was incomplete at the time (34). This paper presents the enzymological properties of an $AroA_{II}$ DAHP synthase that exhibits primary biosynthetic function and represents a distinctive allosteric control pattern.

MATERIALS AND METHODS

Bacterial strains, plasmids, media, and growth conditions. The *Xanthomonas campestris* and *E. coli* strains and plasmids used in this work are listed in Table 1. Growth media for *X. campestris* and *E. coli* included Luria broth (LB) as a complete medium. ARO minimal medium is a modification of the medium reported by Ray et al. (24). It had the following composition (in grams per liter): glucose (1), K_2HPO_4 (7), KH_2PO_4 (2), $(NH_4)_2SO_4$ (0.5), ferric ammonium citrate (0.32), NaCl (0.5), and Casamino Acids (5). After autoclaving, the following compounds (grams per liter) were added: *p*-aminobenzoic acid (0.01), *p*-hydroxybenzoic acid (0.01), 2,3-dihydroxybenzoic acid (0.01), thiamine-HCl (0.0005), and 1 ml of 1 M $MgSO_4$. For induction of the *tac* promoter, IPTG (isopropyl-β-D-thiogalactopyranoside) was added to give a final concentration of 0.2 mM. Ampicillin was used when required at a final concentration of 100 μg/ml.

Materials. Enzymes for molecular genetic applications were purchased from New England BioLabs or Boehringer Mannheim and were used according to the specifications of the manufacturer. Chorismate purified from the accumulation medium of the triple auxotroph *Klebsiella pneumoniae* 62-1 (ATCC 25306) was prepared as the free acid (12) and was 97% pure. $ZnSO_4$, $MgCl_2$, $NiCl_2$, and $MnCl_2$ (puratronic grade) were obtained from Johnson Matthey (Ward Hill, Mass.); other metal salts (reagent grade) were from Sigma (St. Louis, Mo.). EDTA (analytical reagent grade) was purchased as the disodium salt from Mallinckrodt (Paris, Ky.). High-grade Spectra/Por dialysis tubing (VWR) was boiled in 2 mM EDTA and exhaustively washed before use. Chelex-treated water was used for preparation of fresh metal solutions. $FeSO_4$ solutions were always prepared immediately before assays were performed by dissolving it in 0.01 N trace metal grade HCl (Fisher Scientific). Enzyme grade ammonium sulfate was from Sigma.

General DNA techniques and sequencing. Cloning experiments were carried out according to the methods described by Sambrook et al. (27). The DNA sequence of $aroA_{II}$ and flanking 5′ and 3′ regions was determined from plasmid pTacIQ and selected subclones and by primer walking by the dideoxy chain termination procedure (28) using a *Taq* FS dye terminator fluorescence-based cycle sequencing kit (Applied Biosystems) with a Perkin-Elmer/Applied Biosystems Model 377-18E1 sequencer.

Preparation and screening of a genomic DNA library. Total genomic DNA from *X. campestris* was prepared following the method described by Silhavy et al. (31) and was partially digested with *Sau*3AI. Genomic DNA fragments from about 1 to 7 kb in length were isolated from an agarose gel and ligated to *Bam*HI-digested pTacIQ. We had observed that direct transformation of an *X. campestris* genomic library into an McrA and McrB strain resulted in a lower number of transformants than in a strain without an Mcr system. For this reason, the ligation mixture was used to transform the *mcrA mcrCB E. coli* strain XL1 Blue MR. Plasmid DNA from the XL1 Blue MR library was purified and used to transform strain AB3248. Transformants were selected on ARO medium plates containing 100 μg of ampicillin per ml and 0.2 mM IPTG.

Strains and growth of cultures. *E. coli* AB3248, a triple mutant deficient for all three DAHP synthase paralogs, was grown on LB or on minimal medium plus aromatic amino acids required for growth. *E. coli* DH5α and *E. coli* BL21(DE3) were grown on LB plus kanamycin when transformed with a plasmid. *X. campestris* ATCC 33436 (wild type) was grown in either LB or minimal medium supplemented with trace minerals and aromatic amino acids where appropriate.

Clones and plasmids. Plasmid pTacIQ2.3 contains a 6.5-kb DNA segment from *X. campestris*. Plasmid pTacIQ2.3B contains a 2.7-kb fragment of *X. campestris* DNA from plasmid pTacIQ2.3, which carries the gene for DAHP synthase and complementing activities. Plasmid pTacIQ2.3B was used to prepare the pET-24b$^+$ plasmid derivatives pET-M1 and pET-M2 carrying the M1 and M2 clones of DAHP synthase, respectively.

Preparation of clones M1 and M2. Oligonucleotides containing an *Nde*I restriction site were made from the two possible 5′ ATG starts of the DAHP synthase nucleotide sequence, DAHPAI (5′-GATAAACATATGGGTCCGGC TGCGGCCGGCGTC-3′) and DAHPBI (5′-GATAAACATATGTCCGCTTC TTCCCCCTCGAC-3′). An oligonucleotide denoted DAHPSAII with an *Eco*RI

restriction site and corresponding in reverse to the 3′ end of the sequence was also made (5′-GATAAGAATTCCTGCGCAGTCGTTTTGATC-3′). PCRs which included one each of the 5′ oligonucleotides and the 3′ oligonucleotides and the 2.8-kb fragment were performed. The PCR products were gel purified and subjected to digestion with *Nde*I and *Xho*I. The same restriction endonuclease digestion was performed on the pET-24b$^+$ plasmid, which was then purified by gel electrophoresis. The PCR fragments were ligated with the plasmid, transformed into DH5α cells, and spread on LB-kanamycin plates. Several colonies were chosen for analysis. DNA from plasmids containing M1 (pET-M1) and M2 (pET-M2) start sites was purified, subjected to nucleotide sequencing to verify the correct sequence for each, and transformed into BL21(DE3) competent cells to obtain strains designated M1 and M2. A colony from each strain was inoculated into 10 ml of LB-kanamycin for overnight growth at 30°C. These cultures were used to inoculate 10 ml of LB-kanamycin the following morning. IPTG was added when cells reached a density of about 0.6 at A_{600} and were harvested about 2.5 h later. Pellets were used immediately to prepare extracts.

Extract preparation. Cell pellets harvested from M1, M2, *X. campestris*, or *E. coli* AB3248 were suspended into 100 mM potassium phosphate buffer at pH 7.5 containing 1.0 mM DTT, 1.0 mM benzamidine, and 0.1 mM phenylmethylsulfonyl fluoride. Cell suspensions were passed at 18,000 1b/in^2 through a French pressure cell, and the debris was pelleted by centrifugation at 20,000 × *g* for 30 min. Crude extracts to be used for enzyme assays were desalted on 10DG columns (Bio-Rad).

Enzyme assays. DAHP synthase activities were assayed by use of the thiobarbituric acid assay as described before (15). Unless indicated otherwise, assays were carried out at 37°C in 50 mM *N*-(2-hydroxyethyl)piperazine-*N*′-(3-propanesulfonic acid) (EPPS) buffer at pH 8.5.

Enzyme partial purification. For purification, a 0 to 25% ammonium sulfate fraction precipitate was centrifuged in a Sorval centrifuge for 20 min at 4°C. The supernatant fluid was further fractionated to 45% ammonium sulfate and centrifuged. The remaining supernatant was brought to 70% saturation with ammonium sulfate and centrifuged. All pellets were suspended in 50 mM EPPS buffer at pH 8.5, dialyzed for 6 h at 4°C with three buffer changes, and assayed for enzyme activities. Most of the activity was found in the 25 to 45% precipitate fraction, but a small amount was found in the 0 to 25% fraction.

Aliquots of 10 ml from the 25 to 45% ammonium sulfate fractionations were applied to a fast protein liquid chromatography (Amersham Pharmacia Biotech) MonoQ preparative column and washed with 50 mM Epps buffer as described above. A 0 to 0.5 M KCl gradient (70 ml) was applied, and 2-ml fractions were collected. A 1 M step gradient was used to remove all remaining protein. DAHP synthase activity was pooled from tubes which eluted at about the 0.24 M portion of the KCl gradient. This enzyme fraction was used in most of the assays for characterization.

Antibody preparation. Regions from the pretransmembrane sequence (periplasmic) and from the posttransmembrane sequence (cytosolic) of *X. campestris* DAHP synthase were chosen for analysis to determine the best stretch of sequence to use for peptide synthesis and production of antipeptide antibodies. The chosen regions were analyzed by the use of the Network Protein Sequence Analysis at Institut de Biologie et Chimie des Protéines, Lyon, France, to predict antigenic determinants, antigenicity, chain flexibility, and hydrophobic character. After the most favorable sequences for peptide synthesis on each side of the transmembrane region were chosen, they were submitted to Aves Labs, Inc. (Tigard, Oreg.), for further analysis and synthesis. An N-terminal cysteine residue and a spacer amino acid (amino caproic acid) were added to each peptide. These additions allow the use of crude peptide for conjugation purposes and serve to avoid potential problems with steric hindrance.

The synthesized peptides were used to inoculate chickens which lay about one dozen eggs in about 14 days and can produce about 1 g of purified antibody. The highly enriched immunoglobulin fraction from the yolks was then purified (about 500 mg of immunoglobulin Y immune serum antibody). Preimmune serum for use in Western blots and electron microscopy studies was also obtained.

SDS-PAGE and Western blot analysis. Sodium dodecyl sulfate-polyacrylamide gel electrophoresis (SDS-PAGE) was performed with a Mini-Protein II cell (Bio-Rad) by using the method of Laemmli (19). Crude extracts were usually diluted 1:1 (vol/vol) with solubilization buffer and heated to 100°C for 10 min. Whole-cell lysis was performed by resuspending the pellet in 2× SDS sample buffer, vortexing vigorously to shear the chromosomal DNA, and heating to 70°C for about 5 min. Samples ranging from 5 to 10 μl were loaded onto SDS–12% polyacrylamide gels. MultiMark (Novex, San Diego, Calif.) multicolored standards were used as protein markers in order to estimate the efficiency of protein transfer and to determine the molecular weight of proteins of interest.

A Trans-Blot SD semidry transfer cell (Bio-Rad) was used to transfer the protein from the mini-gels to nitrocellulose membranes sandwiched between extra-thick blot-absorbent filter paper (Bio-Rad) layers for about 15 to 30 min. Detection of antigens was performed with a chemiluminescence detection system (*femto*LUCENT; GENO TECH) according to procedures recommended by the manufacturer.

RESULTS

Cloning of a DNA fragment with DAHP synthase activity. The strategy followed to clone the gene coding for DAHP synthase from *X. campestris* was to transform an *E. coli* strain devoid of DAHP synthase activity with a genomic library from *X. campestris*, followed by selection for growth in the absence of exogenous L-tryptophan. *E. coli* strain AB3248 lacks DAHP synthase activity due to mutations that inactivate each of the three genes coding for the differentially regulated paralog isozymes present. This strain is not able to grow in a minimal medium unless all aromatic amino acids and vitamins are added (35).

Chromosomal DNA from *X. campestris* was partially digested with *Sau*3A, ligated into the unique *Bam*HI site present downstream of the *tac* promoter in the expression vector pTacIQ, and transformed into strain XL1 Blue MR. Plasmid DNA purified from this strain was used to transform strain AB3248, which was then plated on ARO minimal medium containing ampicillin (the selecting antibiotic) and IPTG (to induce the *tac* promoter present on plasmid pTacIQ). From about 30,000 CFU, four colonies emerged on the ARO medium plates after 48 h of incubation at 37°C. To test for reversions of any of the DAHP synthase isozyme mutant genes, plasmid DNA was isolated from each of these four transformants and used to retransform strain AB3248. Only one of the plasmids restored growth of strain AB3248 on minimal medium. This plasmid was named pTacIQ2.3. Restriction analysis of the plasmid revealed the presence of a 6.5-kb DNA segment from *X. campestris*. Subcloning experiments showed that a 2.7-kb partial *Bam*HI-derived fragment present in plasmid pTacIQ2.3B was still capable of restoring the growth of strain AB3248 in ARO medium.

One possible open reading frame was deduced but had two possible translation start sites (Fig. 1). The largest (M1) was 478 amino acid residues and would have a calculated pI of 5.94 and a molecular mass of 53.4 kDa. The other (M2) would have a calculated pI of 6.14 and a molecular mass of 51.9 kDa. Both of these were subcloned into vector pET-24b$^+$ (see Materials and Methods) to generate plasmids pET-M1 and pET-M2. These plasmids were introduced into *E. coli* BL21(DE3) to obtain clones M1 and M2.

DAHP synthase in crude extracts. The specific activity of DAHP synthase ($AroA_{II}$) in unfractionated extracts of wild-type *X. campestris* was 5 to 8 nmol/min/mg in 50 mM potassium phosphate buffer at pH 7.0 (36). Distinctly improved specific activities (25.6 ± 1.9 nmol/min/mg) were obtained in 50 mM EPPS buffer at pH 8.3. The pH optimum was broadly similar between pHs of 8.2 and 8.5, dropping sharply under pH 8.2. Significant derepression of $AroA_{II}$ was not observed when a culture in the mid-exponential stage of growth in rich medium was centrifuged and resuspended in minimal medium for 2 h prior to extract preparation. As another approach, a culture in minimal medium was exposed to 10 mM glyphosate to cause starvation for aromatic amino acids (9). Although growth inhibition was observed, derepression of $AroA_{II}$ did not occur.

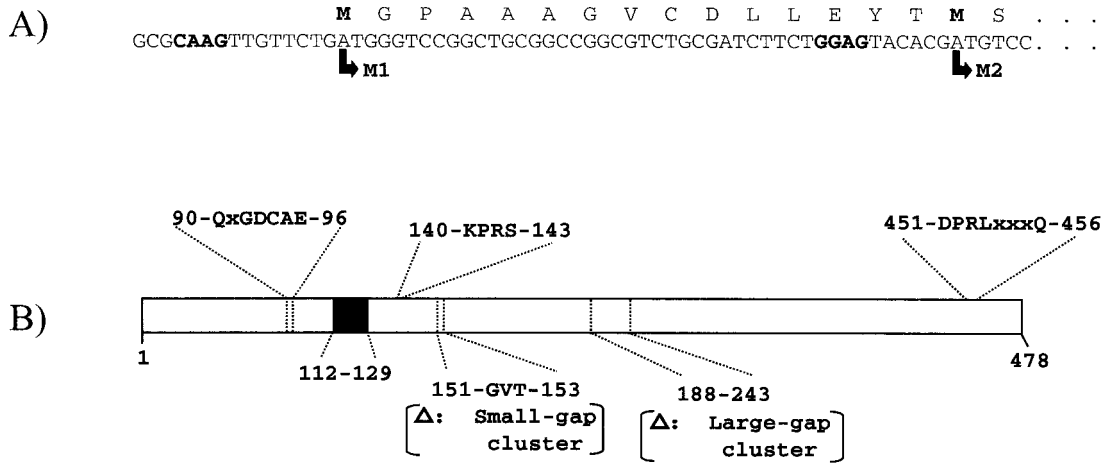

FIG. 1. Sequence features of *X. campestris aroA*$_{II}$ and its gene product AroA$_{II}$. (A) M1 and M2 refer to two possible translation start sites in *aroA*$_{II}$. Putative ribosome-binding sites are highlighted in bold. (B) Schematic of *X. campestris* AroA$_{II}$ protein features. The putative transmembrane region (residues 112 to 129) is shown in black. The location of the conserved KPRT/S motif is shown. Conserved motifs present in the putative periplasmic region and in the carboxy-terminal region are shown (x denotes nonconserved residues). *X. campestris* residue numbers which correspond to deletions (△) conserved in the phylogenetic groupings indicated in Fig. 3 are shown. The large-gap cluster of organisms possesses 15 to 20 of the amino acid residues within the region corresponding to residues 188 to 243 of *X. campestris*, but these are not highly conserved.

Hence, the enzyme may not be subject to repression control by amino acid end products.

Crude extracts prepared from the *E. coli* BL21(DE3) clones M1 and M2 exhibited elevated specific activities of 796 and 3,109 nmol/min/mg, respectively. Thus, compared to the wild type, the level of AroA$_{II}$ in the M2 clone was enriched 25-fold or more. A preliminary series of assays comparing the enzymological properties of unfractionated extracts from the wild-type, M1, and M2 strains was undertaken to assess possible differences in catalytic properties, temperature optimum, pH optimum, and divalent cation requirements or in sensitivity to allosteric effectors. The background DAHP synthases that were present in *E. coli* BL21(DE3) clones were minimized by their repression to low levels in LB and the use of phenylalanine and tyrosine to inhibit the major *E. coli* paralogs. Characterization of the *X. campestris* AroA$_{II}$ protein in the *E. coli* AB3248 transformant was, of course, uncomplicated by any background of *E. coli* enzymes. We showed that purified *E. coli* tryptophan-sensitive DAHP available in our laboratory separated completely from *X. campestris* AroA$_{II}$ during the first step of purification. No significant differences between M1 and M2 were found. Multiple alignment results were consistent with the probability that clone M2 possesses the authentic translation start site since the length of clone M2 corresponded best with its nearest relatives, e.g., AroA$_{II}$ from *Helicobacter pylori* or from *Pseudomonas aeruginosa*. The initial conservation observed at the N terminus of clone M2 was 16-WSPQSW-21, which corresponded with 6-WSPTSW-11 of *H. pylori* and 5-WSPESW-10 of *P. aeruginosa*. AroA$_{II}$ from the M2 clone therefore seemed to be the most appropriate protein for use in detailed studies.

Crude extracts from both wild-type *X. campestris* and from the M1 or M2 clone in *E. coli* were stable at −70°C for at least 2 months. When aliquots of M2 extract that had been diluted 100-fold in 50 mM EPPS buffer (pH 8.5) were compared with aliquots diluted 100-fold in potassium phosphate buffer at pH 7.5, the latter preparations were significantly more stable in storage at −70°C. In EPPS buffer the half-life was about 4 days compared to about 24 days in phosphate buffer.

Partial purification. Characterization of AroA$_{II}$ was carried out in EPPS buffer, the optimum buffer for catalysis. This exacerbated the problem encountered with stability, AroA$_{II}$ being increasingly unstable with increasing purification or increasing dilution. No stabilizing conditions or agents were found, except for a modest effect of 30% glycerol. However, glycerol was not used because of interference with the chemical assay for DAHP.

In order to deal with the stability problem, a 1-day purification method was worked out for the enzymological characterization of AroA$_{II}$ from the M2 clone. Unfractionated extract (see Materials and Methods) was subjected to ammonium sulfate fractionation. Ninety-nine percent of the activity salted out in the 25 to 45% $(NH_4)_2SO_4$ fraction. An assay after resolubilization and dialysis showed an excellent 10-fold purification (266 ± 14 nmol/min/mg). Application to an anion-exchange column yielded fractions which exhibited an additional purification of about ninefold (2.40 ± 0.16 μmol/min/mg). This protocol gave consistent preparations for characterization studies. A single major band was visualized after SDS-PAGE, but multiple minor bands were seen when the gel was overloaded. Western blots confirmed the presence of a single major band of the expected molecular weight. Further attempts to purify the enzyme from gel filtration columns were unsuccessful. Exposure of enzyme preparations, either crude *X. campestris* extracts or purified protein, to antibody resulted in greater than 99% inhibition of DAHP synthase activity.

Temperature optimum. Preliminary experiments indicated that AroA$_{II}$ exhibited a temperature optimum in the range of 50 to 56°C. Detailed assays were carried out in this range to locate the highest temperature at which proportionality was

TABLE 2. Reactivation of EDTA-inactivated *X. campestris* $AroA_{II}$ by divalent metals[a]

Addition(s)	% Control activity
None	100
EDTA	12
EDTA + $MgCl_2$	17
EDTA + $MnCl_2$	78
EDTA + $CoCl_2$	109
EDTA + $CaCl_2$	13
EDTA + $FeCl_2$	7
EDTA + $ZnSO_4$	96
EDTA + $CuSO_4$	7
EDTA + $NiCl_2$	63

[a] EDTA (0.2 mM) and a 0.5 mM concentration of the indicated metal salt were added to an assay mixture containing 13 μg of partially purified *X. campestris* $AroA_{II}$ and incubated for 4 min at 37°C.

maintained throughout the duration of the 4-min assays used. The temperature optimum was 52°C.

The energy of activation determined according to the Arrhenius equation from a plot of log V (velocity) versus the reciprocal of the temperature (Kelvin scale) was calculated from the negative slope $-E/R$ (E is activation energy and R is the gas constant) and had a value of 11.9 ± 0.9 kcal mol^{-1}.

Effect of DTT. Since $AroA_{II}$ from higher plants is hysteretically activated by DTT (7, 11), the possible activation of *X. campestris* $AroA_{II}$ by DTT was examined in all strains studied and at different stages of purification. No effect of DTT was found with active preparations. Preparations that had lost some or all of the original activity were also examined, but reactivation by DTT was not found.

Effect of divalent metals. Neither unfractionated nor partially purified extracts were affected by the presence of divalent metals, as previously noted (36). However, EDTA was a potent inhibitor and was able to completely inactivate the M2 enzyme. Inhibition by EDTA was essentially instantaneous. EDTA was not able to strip essential divalent metal moieties from *X. campestris* $AroA_{II}$, since dialysis of a completely inhibited preparation restored all (107%) of the original activity.

A variety of divalent metals were able to reactivate *X. campestris* $AroA_{II}$ (Table 2). Similar results were obtained regardless of whether the enzyme was exposed to EDTA or the divalent metal first or whether EDTA and the test metal were added simultaneously. Co^{2+}, Zn^{2+}, and Ni^{2+} were the most effective metal additives, at 0.5 mM.

Kinetic properties of *X. campestris* $AroA_{II}$. A series of substrate saturation curves were generated at different fixed concentrations of each substrate, using elapsed reaction times of 4 min at 37°C. Conditions of proportionality were maintained with respect to reaction time and protein concentration. Replots of data obtained from double-reciprocal plots resulted in apparent K_m values of 0.23 and 0.13 mM for E4P and PEP, respectively.

Analysis of inhibition data confirmed the results of Whitaker et al. (36) that chorismate competitively inhibited each substrate, whereas L-tryptophan was a noncompetitive inhibitor of each substrate. Calculated K_i values for chorismate were 0.31 mM (for PEP) and 0.09 mM (for E4P). Calculated K_i values for L-tryptophan were 0.35 mM (for PEP) and 0.61 mM (for E4P).

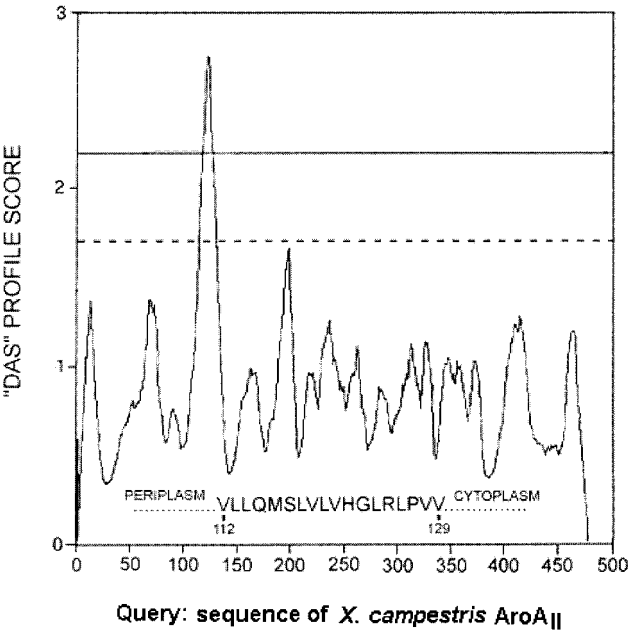

FIG. 2. Putative transmembrane region of *X. campestris* $AroA_{II}$. The graphical output shown was produced by a program which applies the dense alignment surface (DAS) method (6). A dashed horizontal line indicates the loose cutoff and a solid horizontal line refers to the strict cutoff. The sequence corresponding to the transmembrane region is shown at the bottom.

Transmembrane region. When the *X. campestris* $AroA_{II}$ sequence was subjected to PSORT analysis (http://psort.nibb.ac.jp), an affirmative result was obtained for a single transmembrane region that would span the inner membrane (Fig. 1). Figure 2 illustrates the 18-amino-acid region predicted to span the inner membrane by the dense alignment surface method. This would place the N-terminal 111 amino acid residues in the periplasm and the C-terminal 349 residues in the cytoplasm. Similar results were obtained for most of the sequences belonging to the upper group shown in Fig. 3. In contrast, members of the lower group were uniformly predicted to be cytoplasmic proteins by application of the PSORT program. The two *P. aeruginosa* paralogs illustrate these $AroA_{II}$ differences in a common organism. The biosynthetic pathway protein (upper sequence in Fig. 3) has 448 residues, of which residues 87 to 103 are predicted (certainty of 0.223) to span the inner membrane. The phenazine pathway paralog (lower sequence in Fig. 3) has 405 residues and is predicted to be cytoplasmic, with a certainty of 0.480.

KPRS motif of $AroA_{II}$. Elucidation of the crystal structure of the phenylalanine-sensitive paralog of $AroA_I$ (29) reveals that the crucial amino acid residues which coordinate with metal, PEP, and E4P are scattered throughout the primary sequence between C_{61} and D_{326}. The most compact array of crucial *E. coli* $AroA_I$ residues is the motif 97-KPRT-100. K_{97} is bridged by water to a divalent metal and also coordinates with the carboxylate moiety of PEP. R_{99} is inferred to be an E4P-coordinating residue. The $AroA_{II}$ family enzymes all share a very similar motif (140-KPRS-143 in *X. campestris*). The nearby *E. coli* $AroA_I$ residue R_{92}, which coordinates with PEP,

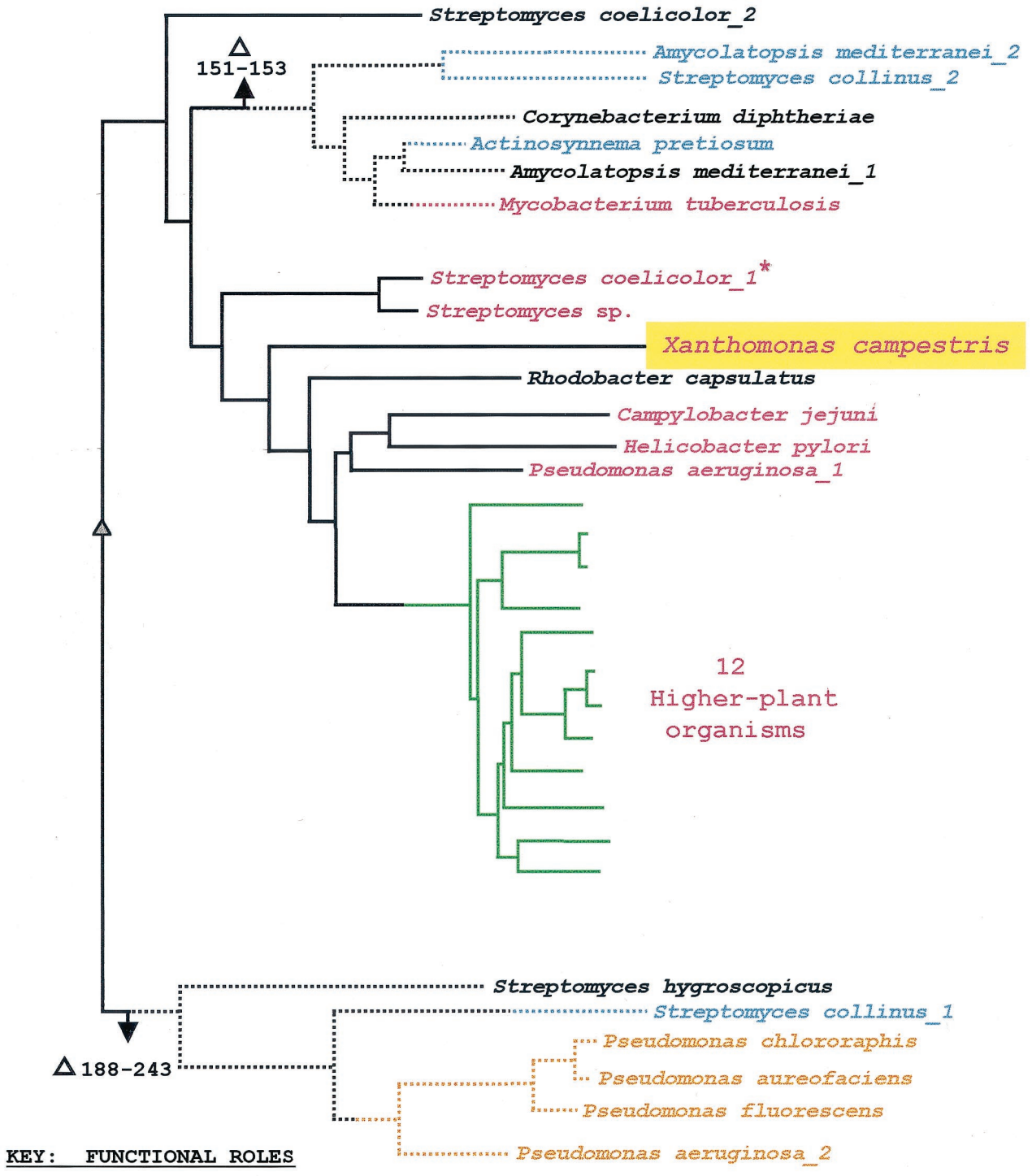
Streptomyces coelicolor_2
151-153
Amycolatopsis mediterranei_2
Streptomyces collinus_2
Corynebacterium diphtheriae
Actinosynnema pretiosum
Amycolatopsis mediterranei_1
Mycobacterium tuberculosis
Streptomyces coelicolor_1*
Streptomyces sp.
Xanthomonas campestris
Rhodobacter capsulatus
Campylobacter jejuni
Helicobacter pylori
Pseudomonas aeruginosa_1
12
Higher-plant
organisms
Streptomyces hygroscopicus
Streptomyces collinus_1
Pseudomonas chlororaphis
Pseudomonas aureofaciens
Pseudomonas fluorescens
188-243
Pseudomonas aeruginosa_2
KEY: FUNCTIONAL ROLES
AminoDAHP synthase
Primary amino acid biosynthesis
Phenazine pigment
Uncertain

may be equivalent to *X. campestris* R_{133}, which is completely conserved in $AroA_{II}$ proteins.

Another motif of interest is *E. coli* $AroA_I$ 265-DxxHxN-270, from which H_{268} coordinates with both PEP and divalent metals. The *X. campestris* $AroA_{II}$ motif 374-DxxHxN-379 may be a functional equivalent since this motif is conserved throughout the $AroA_{II}$ family.

DISCUSSION

Comparison of *X. campestris* $AroA_{II}$ with higher-plant-type $AroA_{II}$. The plastid-localized $AroA_{II}$ in higher plants (denoted DS-Mn) was the first $AroA_{II}$ species to be extensively characterized. All higher-plant-type $AroA_{II}$ proteins share a number of distinctive properties (7, 8, 22). Since the microbial and higher-plant-type $AroA_{II}$ proteins exhibit relatively high amino acid sequence identities, it was of interest to determine what properties of plant $AroA_{II}$ might also typify *X. campestris* $AroA_{II}$. Both proteins function in primary aromatic amino acid biosynthesis, and it was shown that in each case (8, 36) a single enzyme species is tightly regulated via an allosteric pattern of control called sequential feedback inhibition (16). However, plant $AroA_{II}$ and *X. campestris* $AroA_{II}$ recognize different key allosteric effectors, L-arogenate and chorismate, respectively. This reflects different biochemical pathway steps diverging from prephenate in these organisms (36). The minor sensitivity of *X. campestris* $AroA_{II}$ to inhibition by L-tryptophan is paralleled by a similar sensitivity noted for plant $AroA_{II}$ in at least one case (mung bean) (26). $AroA_{II}$ from either source is quite labile and exhibits a relatively high temperature optimum. The putative transmembrane region of *X. campestris* $AroA_{II}$ aligned with a hydrophobic region in higher plants, which may also be a transmembrane region. In contrast to the aforementioned similarities, a number of striking differences are also apparent.

Higher-plant-type $AroA_{II}$ exhibits dramatic hysteretic activation by DTT and is thought to be under redox control influenced by endogenous thioredoxin (11). *X. campestris* $AroA_{II}$ was not affected by DTT, and inactive enzyme preparations could not be rejuvenated with DTT. In addition, whereas higher-plant-type $AroA_{II}$ displays sigmoid substrate saturation curves with respect to either E4P or PEP, *X. campestris* $AroA_{II}$ produced straightforward first-order kinetics.

Higher-plant-type $AroA_{II}$ has activity in the absence of added metal and is stimulated about 50% with the addition of 0.5 mM Mn^{2+}. The enzyme is readily stripped free of metal by EDTA treatment to give an inactive preparation which can be restored to original activity levels by Ca^{2+}. It has been suggested (8) that two metal-binding sites may exist, one binding either Ca^{2+} or Mn^{2+} and the other binding only Mn^{2+}. In contrast, although *X. campestris* $AroA_{II}$ is also active in the absence of added metals, further metal additions do not stimulate activity. Thus, *X. campestris* $AroA_{II}$ seems to be saturated with firmly bound metal. While EDTA is effective as an inhibitor of activity, it is not able to strip the metal from the enzyme. Mn^{2+} was able to displace the EDTA-metal complex from the *X. campestris* $AroA_{II}$, but Ca^{2+} was ineffective and Co^{2+} and Zn^{2+} were superior to Mn^{2+}.

The $AroA_{II}$ protein is probably conserved throughout the *Xanthomonas* genus since *Xanthomonas hyacinthi* (strain ICPB-XH110) was previously reported (13) to possess a DAHP synthase that was 88% inhibited by 0.07 mM chorismate and 33% inhibited by 0.07 mM L-tryptophan.

Independent evolution of tryptophan-inhibited AroA enzymes. With respect to microbial AroA enzymes that are sensitive to feedback inhibition by L-tryptophan, three classes have been recognized by this criterion (1). First, DS-TRP (exemplified by *E. coli*) is exclusively subject to inhibition by L-tryptophan. Second, DS-TRP(cha) recognizes L-tryptophan as a major inhibitor and chorismate as a minor inhibitor (exemplified by *P. aeruginosa*). Third, DS-CHA(trp) recognizes chorismate as a major inhibitor and L-tryptophan as a minor inhibitor. It was proposed (1) that the DS-TRP(cha) gene might have arisen from a fusion between genes encoding an ancestral feedback-insensitive AroA and the large subunit of anthranilate synthase, the latter providing a single source of binding sites for both chorismate and L-tryptophan. Since anthranilate synthase is an aminase, this idea is even more intriguing for the amino-DAHP synthase class of $AroA_{II}$ (Fig. 3), which introduces an amino group into the reaction (17). However, entry of various $AroA_{II}$ sequences as queries in PSI-BLAST (National Center for Biotechnology Information) did not return hits for anthranilate synthase.

Since the tryptophan-sensitive *E. coli* $AroA_I$ protein belongs to a homolog class different from that of tryptophan-sensitive members of $AroA_{II}$, it had an independent origin as a paralog member of the $AroA_I$ family. It is interesting that both *E. coli* and *N. crassa* possess three differentially controlled isoenzymes of DAHP synthase (14), but whereas *E. coli* expresses three paralogs of $AroA_I$, *N. crassa* expresses two paralogs of $AroA_I$ (phenylalanine and tyrosine regulated) and one of $AroA_{II}$

FIG. 3. Phylogenetic tree of plant-type ($AroA_{II}$) DAHP synthases. A multiple alignment obtained with the Multalin program was analyzed by the neighbor-joining method using the Phylip program. The higher-plant proteins (lineage lines shown in green) are tightly clustered, form a nested set within a more divergent cluster of microbial proteins, and are most closely related to orthologs within the gram-negative bacteria. The position of the *X. campestris* protein is highlighted in yellow. The positions of the $AroA_{II}$ proteins from *M. avium* and *M. leprae* (not shown) are almost identical to that shown for *M. tuberculosis*. The two *Stigmatella aurantiaca* $AroA_{II}$ proteins (Fig. 4) are not shown, but both are close homologs of *P. aeruginosa*_1 $AroA_{II}$. The most outlying group of $AroA_{II}$ proteins include those (color-coded orange) which in the *Pseudomonas* species shown are functionally linked to phenazine biosynthesis in the stationary phase of growth. The groupings marked with dotted lines and referred to as the small-gap cluster and the large-gap cluster in Fig. 1 are defined by the conserved deletions shown. Proteins are denoted in magenta in cases where complete genomic sequencing or other evidence supports the conclusion that $AroA_{II}$ is the sole enzyme for primary aromatic amino acid biosynthesis. Of the two $AroA_{II}$ proteins from *Streptomyces coelicolor* in the database, the one studied by Walker et al. (34) can be identified from their peptide sequencing and is denoted with an asterisk. The latter enzyme functions in primary amino acid biosynthesis since it was the only species detected during active growth. The *P. aeruginosa*_1 $AroA_{II}$ DAHP synthase is undoubtedly a member of the DS-TRP(cha) class of tryptophan- and chorismate-sensitive enzymes (1). Variant $AroA_{II}$ proteins that function as amino-DAHP synthases and that are known to function in ansamycin antibiotic production are shown in blue.

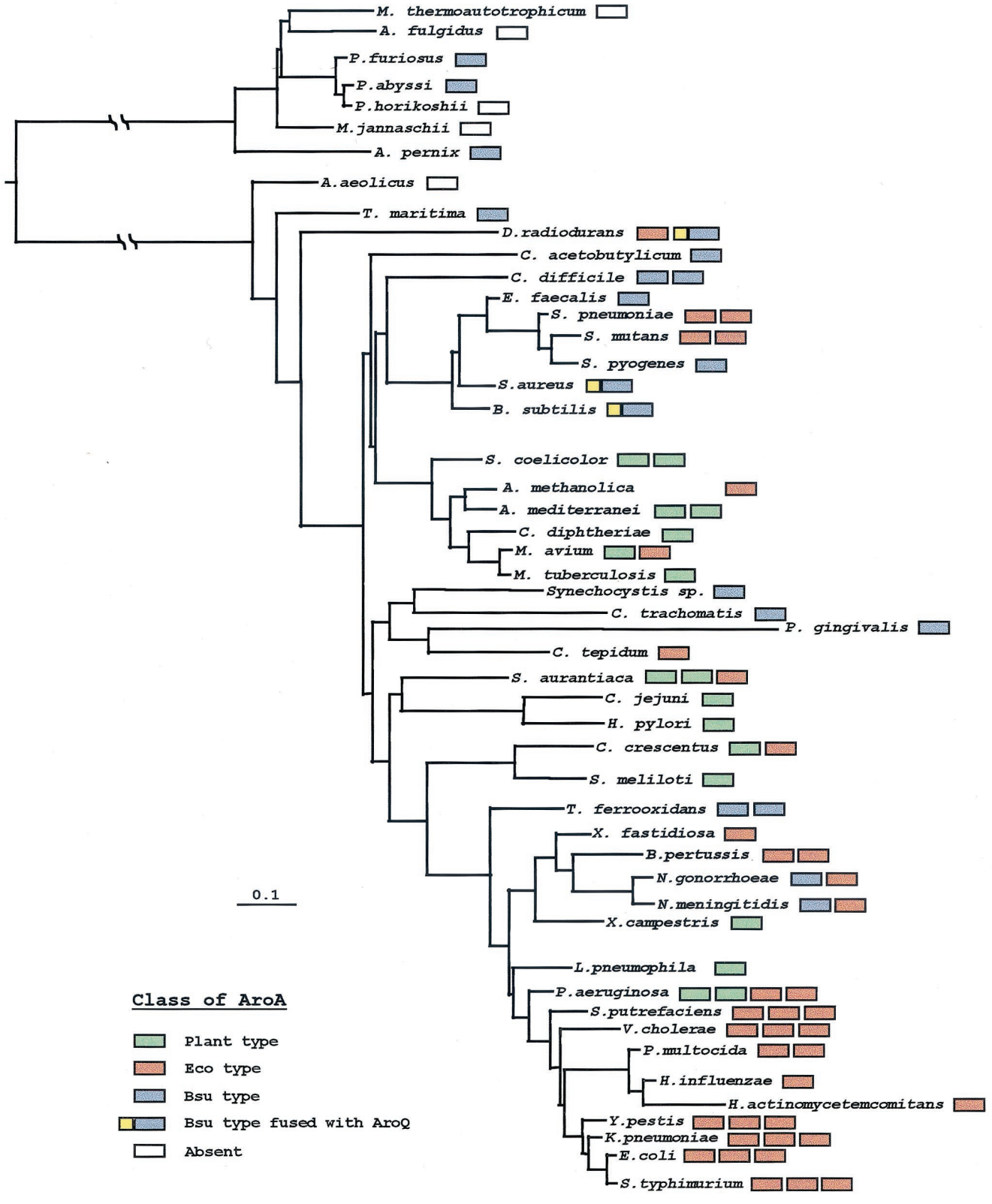
M. thermoautotrophicum
A. fulgidus
P.furiosus
P.abyssi
P.horikoshii
M.jannaschii
A. pernix
A.aeolicus
T. maritima
D.radiodurans
C. acetobutylicum
C. difficile
E. faecalis
S. pneumoniae
S. mutans
S. pyogenes
S.aureus
B. subtilis
S. coelicolor
A. methanolica
A. mediterranei
C. diphtheriae
M. avium
M. tuberculosis
Synechocystis sp.
C. trachomatis
P. gingivalis
C. tepidum
S. aurantiaca
C. jejuni
H. pylori
C. crescentus
S. meliloti
T. ferrooxidans
X. fastidiosa
B.pertussis
N.gonorrhoeae
N.meningitidis
X.campestris
L.pneumophila
P.aeruginosa
S.putrefaciens
V.cholerae
P.multocida
H.influenzae
H.actinomycetemcomitans
Y.pestis
K.pneumoniae
E.coli
S.typhimurium
0.1
Class of AroA
Plant type
Eco type
Bsu type
Bsu type fused with AroQ
Absent

(tryptophan regulated). Thus, these classic three-isoenzyme systems, which exhibit a similar functional pattern, differ in that the tryptophan-regulated enzymes had independent evolutionary origins.

$AroA_{II}$ proteins have a microbial origin. Figure 3 shows that $AroA_{II}$ proteins from higher plants are highly conserved and are nested inside a larger and less conserved (more ancient) microbial grouping. The most closely related sequences of the *Bacteria* include species of *Pseudomonas, Campylobacter, Rhodobacter*, and *Xanthomonas*. Although it has been suggested that members of the *Bacteria* domain might have acquired $AroA_{II}$ from higher plants (21), the tree shown in Fig. 3 clearly reveals an ancient origin of this AroA family within the *Bacteria*. Thus, acquisition of $AroA_{II}$ by higher plants probably occurred relatively recently via endosymbiosis from a donor in the gram-negative lineage of the *Bacteria*.

Figure 3 shows a clear dichotomy of $AroA_{II}$ sequences, although this is not necessarily a functional dichotomy. The lower cluster of $AroA_{II}$ proteins is engaged in phenazine pigment production (8, 23) or antibiotic production. In the latter case, *Streptomyces hygroscopicus* uses a derivative of DAHP for synthesis of a polyketide starter for rapamycin biosynthesis (25) and *Streptomyces collinus* utilizes an $AroA_{II}$ species which produces amino-DAHP as a precursor of 3-amino, 5-hydroxybenzoate, a starter unit for napthomycin (5). These proteins lack the putative transmembrane region, are probably not sensitive to inhibition by chorismate or L-tryptophan, and are encoded by genes belonging to operons whose expression is induced during stationary-phase metabolism. These tend to be the smallest $AroA_{II}$ proteins, probably because of the deletion of the majority of residues within the region corresponding to *X. campestris* residues 188 to 243 (Fig. 2). Given the deletion of this region in proteins presumed to lack allosteric control and the variability of this region in organisms recognizing different allosteric effectors, the region corresponding to *X. campestris* residues 188 to 243 may very well dictate allosteric specificity. (Although the *S. collinus* sequence is about 100 amino acids longer than other members of the lower cluster, these amino acids are accounted for as N- and C-terminal extensions. It may very well be that the true translational start is a GTG codon that corresponds to residue 68 of the current database entry.)

The upper cluster possesses a number of $AroA_{II}$ proteins which presumably catalyze the formation of amino-DAHP as a precursor of ansamycin antibiotics (3, 5). Since the $AroA_{II}$ protein designated *Amycolatopsis mediterranei*_1 functions as an amino-DAHP synthase, the other, designated *A. mediterranei*_2, could serve in primary biosynthesis. However, this is not a complete genome, and we note that the $AroA_{I}$ class of DAHP synthases has been reported in other species of *Amycolatopsis* (2, 33).

A number of $AroA_{II}$ proteins in Fig. 3 are from organisms whose genomes have been sequenced. *Mycobacterium tuberculosis, Campylobacter jejuni*, and *H. pylori* all possess a single DAHP synthase of the $AroA_{II}$ type (Fig. 4). It is likely that *Corynebacterium diphtheriae* (and *X. campestris*) also possesses a single species of DAHP synthase (i.e., $AroA_{II}$). Hence, these $AroA_{II}$ proteins must function in primary biosynthesis. Particular enzyme reactions can be performed by enzymes which evolved independently and have been referred to as analogous enzymes (10). The frequency of analog proteins which correspond to a given function is surprisingly high (10). It seems quite possible that $AroA_{II}$ of *X. campestris* may have originally functioned as an enzyme of secondary metabolism, reminiscent of many contemporary $AroA_{II}$ enzymes. Chorismate-binding ability might have been a fortuitous property of the enzyme which was subsequently exploited to provide a mechanism of sequential feedback inhibition. Either this facilitated the loss of a less efficient coexisting $AroA_{I}$ analog, or prior loss of the latter created selective pressure for recruitment of the $AroA_{II}$ analog to primary biosynthetic function.

Phylogenetic distribution of $AroA_{II}$ proteins. If the 16S rRNA tree is accepted as a gauge of phylogenetic breadth, $AroA_{II}$ clearly exhibits the most narrow phylogenetic distribution of the three groups of AroA proteins (Fig. 4). Thus, it must have the most recent origin. It may have arisen in association with a specialized function for secondary metabolism. Within *Mycobacterium, Mycobacterium avium* possesses both $AroA_{I\alpha}$ and $AroA_{II}$, whereas both *Mycobacterium tuberculosis* and *Mycobacterium bovis* possess only $AroA_{II}$. We suggest that $AroA_{I\alpha}$ was the original enzyme serving aromatic biosynthesis in *Mycobacterium* and has since been replaced by $AroA_{II}$. Accordingly, $AroA_{I\alpha}$ has been lost in *M. tuberculosis* and in *M. bovis*, and it may essentially be an evolutionary remnant in *M. avium*.

Figure 4 shows that a number of organisms other than *X. campestris* rely on $AroA_{II}$ as the sole enzyme available for aromatic amino acid biosynthesis. Although some of these organisms are nutritionally fastidious, the presence of genes specifying complete pathways to aromatic amino acids indicates the presence of a functional pathway. In addition to *M. tuberculosis* (and *M. bovis*), these include *C. jejuni, H. pylori, Sinorhizobium meliloti*, and *Legionella pneumophila*. Since DAHP synthase is a crucial focal point of allosteric regulation

FIG. 4. Distribution of AroA homology types in organisms whose positions are shown on a 16S rRNA-based tree. A subtree was obtained from the Ribosomal Database site (http://www.cme.msu.edu.rdp/). Each bar is color coded to identify any of the three types of DAHP synthase, as keyed in the legend. The plant type, Eco type, and Bsu type correspond to $AroA_{II}$, $AroA_{I\alpha}$, and $AroA_{I\beta}$ (see the introduction). Multiple bars of the same color correspond to paralogs. Fusions that have resulted in attached AroQ (chorismate mutase) domains are shown in yellow. In some cases no AroA homology type is discernible (open bars). The two *Neisseria* Bsu type $AroA_{I\beta}$ proteins lack the highly conserved motif KPRT; therefore, the coding DNA sequences can be considered pseudogenes. Listing of genera from top to bottom: *Methanobacterium, Archaeoglobus, Pyrococcus* (three species), *Methanococcus, Aeropyrum, Aquifex, Thermotoga, Deinococcus, Clostridium* (two species), *Enterococcus, Streptococcus* (three species), *Staphylococcus, Bacillus, Streptomyces, Amycolatopsis* (two species), *Corynebacterium, Mycobacterium* (two species), *Synechocystis, Chlamydia, Porphyromonas, Chlorobium, Stigmatella, Campylobacter, Helicobacter, Caulobacter, Sinorhizobium, Thiobacillus, Xylella, Bordetella, Neisseria* (two species), *Xanthomonas, Legionella, Pseudomonas, Shewanella, Vibrio, Pasteurella, Haemophilus* (two species), *Yersinia, Klebsiella, Escherichia*, and *Salmonella*.

(albeit with remarkable variation of control patterns), one would assume that $AroA_{II}$ in these organisms is subject to sequential feedback inhibition as in *Xanthomonas* (via chorismate) or higher plants (via L-arogenate).

ACKNOWLEDGMENTS

We thank A. Van Kimmenade (Genencor International, Palo Alto, Calif.) for kindly providing plasmid pTacIQ and Gary Xie (Los Alamos National Laboratory) for assistance with phylogenetic analysis.

G.G. was supported by a fellowship from Dirección General de Asuntos del Personal Académico de la Universidad Nacional Autónoma de México.

ADDENDUM IN PROOF

Recently, Birck and Woodward (M. R. Birck and R. W. Woodward, J. Mol. Evol. **52:**205–214, 2001) published a phylogenetic tree that placed two higher-plant $AroA_{II}$ sequences with members of both the $AroA_{I\alpha}$ and $AroA_{I\beta}$ subfamilies, with the inference that $AroA_{II}$ and $AroA_{I\alpha}$ belong to a common "class." However, any tree-building program will fail to produce a valid tree without input of a proper multiple alignment. Although a few common motifs might exist (see above), there is not currently any alignment available that would provide sufficient acceptable matches for entry into a tree-building program, particularly with the large gaps that would be necessary due to the great size difference of the $AroA_I$ and $AroA_{II}$ protein families.

REFERENCES

1. **Ahmad, S., B. Rightmire, and R. A. Jensen.** 1986. Evolution of the regulatory isozymes of 3-deoxy-D-*arabino*-heptulosonate 7-phosphate synthase present in the *Escherichia coli* genealogy. J. Bacteriol. **165:**146–154.
2. **Alves, A. M., W. G. Meijer, J. W. Vrijbloed, and L. Dijkhuizen.** 1996. Characterization and phylogeny of the *pfp* gene of *Amycolatopsis methanolica* encoding Ppi-dependent phosphofructokinase. J. Bacteriol. **178:**149–155.
3. **August, P. R., L. Tang, Y. J. Yoon, S. Nig, R. Muller, T. W. Yu, M. Taylor, D. Hoffmann, C. G. Kim, X. Zhang, C. R. Hutchinson, and H. G. Floss.** 1998. Biosynthesis of the ansamycin antibiotic rifamycin: deductions from the molecular analysis of the *rif* biosynthetic gene cluster of *Amycolatopsis mediterranei* S699. Chem. Biol. **2:**69–79.
4. **Bentley, R.** 1990. The shikimate pathway: a metabolic tree with many branches. Crit. Rev. Biochem. Mol. Biol. **5:**307–384.
5. **Chen, S., D. von Bamberg, V. Hale, M. Breuer, B. Hardt, R. Muller, H. G. Floss, K. A. Reynolds, and E. Leistner.** 1999. Biosynthesis of *ansatrienin* (*mycotrienin*) and *napthomycin*. Identification and analysis of two separate biosynthetic gene clusters in *Streptomyces collinus* Tu 1892. Eur. J. Biochem. **1:**98–107.
6. **Cserzo, M., E. Wallin, I. Simon, G. von Heijne, and A. Elofsson.** 1997. Prediction of transmembrane alpha-helices in prokaryotic membrane proteins: the dense alignment surface method. Protein Eng. **6:**673–676.
7. **Doong, R. L., and R. A. Jensen.** 1992. Synonymy of the three apparent isoenzymes of 3-deoxy-D-*arabino*-heptulosonate 7-phosphate synthase in *Pisum sativum* L. with 3-deoxy-D-*manno*-octulosonate 8-phosphate synthase and the DS-Co/DS Mn isoenzyme pair. New Phytol. **121:**165–171.
8. **Doong, R. L., R. J. Ganson, and R. A. Jensen.** 1993. Plastid-localized 3-deoxy-D-*arabino*-heptulosonate 7-phosphate synthase (DS Mn): the early-pathway target of sequential feedback inhibition in higher plants. Plant Cell Environ. **16:**393–402.
9. **Fischer, R. S., A. Berry, C. G. Gaines, and R. A. Jensen.** 1986. Comparative action of glyphosate as a trigger of energy drain in eubacteria. J. Bacteriol. **168:**1147–1154.
10. **Galperin, M. Y., D. R. Walker, and E. V. Koonin.** 1998. Analogous enzymes: independent inventions in enzyme evolution. Genome Res. **8:**779–790.
11. **Ganson, R. J., T. A. d'Amato, and R. A. Jensen.** 1986. The two-isozyme system of 3-deoxy-D-*arabino*-heptulosonate 7-phosphate synthase in *Nicotiana silvestris* and other higher plants. Plant Physiol. **82:**203–210.
12. **Gibson, F.** 1964. Chorismic acid: purification and some chemical and physical studies. Biochem. J. **90:**256–261.
13. **Jensen, R. A., D. S. Nasser, and E. W. Nester.** 1967. Comparative control of a branch-point enzyme in microorganisms. J. Bacteriol. **94:**1582–1593.
14. **Jensen, R. A., and D. S. Nasser.** 1968. Comparative regulation of isoenzymic 3-deoxy-D-*arabino*-heptulosonate 7-phosphate synthetases in microorganisms. J. Bacteriol. **95:**188–196.
15. **Jensen, R. A., D. H. Calhoun, and S. L. Stenmark.** 1973. Allosteric inhibition of 3-deoxy-D-*arabino*-heptulosonate 7-phosphate synthetase by tyrosine, tryptophan and phenylpyruvate in *Pseudomonas aeruginosa*. Biochim. Biophys. Acta. **293:**256–268.
16. **Jensen, R. A., and E. W. Nester.** 1965. The regulatory significance of intermediary metabolites: control of aromatic acid biosynthesis by feedback inhibition in *Bacillus subtilis*. J. Mol. Biol. **12:**468–481.
17. **Kim, C., A. Kirschning, P. Bergon, P. Zhou, E. Su, B. Sauerbrei, S. Ning, Y. Ahn, M. Breuer, E. Leistner, and H. G. Floss.** 1996. Biosynthesis of 3-amino-5-hydroxybenzoic acid, the precursor of mC_7N units in ansamycin antibiotics. J. Am. Chem. Soc. **118:**7486–7491.
18. **Kim, C., T. Yu, C. B. Fryhle, S. Handa, and H. G. Floss.** 1998. 3-Amino-5-hydroxybenzoic acid synthase, the terminal enzyme in the formation of the precursor of mC_7N units in rifamycin and related antibiotics. J. Biol. Chem. **273:**6030–6040.
19. **Laemmli, U. K.** 1970. Cleavage of structural proteins during the assembly of the head of bacteriophage T4. Nature **227:**680–685.
20. **Liev, K. W., and A. M. Alvarez.** 1981. Biological and morphological characterization of *Xanthomonas campestris* bacteriophages. Phytopathology **71:** 269–273.
21. **Mavrodi, D. V., V. M. Ksenzenko, R. F. Bonsall, R. J. Cook, A. M. Boronin, and L. S. Thomashow.** 1998. A seven-gene locus for synthesis of phenazine-1-carboxylic acid by *Pseudomonas fluorescens* 2–79. J. Bacteriol. **180:**2541–2548.
22. **Morris, P. F., R. L. Doong, and R. A. Jensen.** 1989. Evidence from *Solanum tuberosum* in support of the dual-pathway hypothesis of aromatic biosynthesis. Plant Physiol. **89:**10–14.
23. **Pierson, L. S., T. Gaffney, S. Lam, and F. Gong.** 1995. Molecular analysis of genes encoding phenazine biosynthesis in the biological control bacterium *Pseudomonas aureofaciens* 30–84. FEMS Lett. **134:**299–307.
24. **Ray, J. M., C. Yanofsky, and R. Bauerle.** 1988. Mutational analysis of the catalytic and feedback sites of the tryptophan-sensitive 3-deoxy-D-*arabino*-heptulosonate 7-phosphate synthase of *Escherichia coli*. J. Bacteriol. **170:** 5500–5506.
25. **Ruan, X., D. Stassi, S. A. Lax, and L. Katz.** 1997. A second type-I PKS gene cluster isolated from *Streptomyces hygroscopicus* ATCC 29253, a rapamycin-producing strain. Gene **203:**1–9.
26. **Rubin, J. L., and R. A. Jensen.** 1985. Differentially regulated isozymes of 3-deoxy-D-*arabino*-heptulosonate 7-phosphate synthase from seedlings of *Vigna radiata* [L.] Wilczek. Plant Physiol. **79:**711–718.
27. **Sambrook, J., E. F. Fritsch, and T. Maniatis.** 1989. Molecular cloning: a laboratory manual, 2nd ed. Cold Spring Harbor Laboratory Press, Cold Spring Harbor, N.Y.
28. **Sanger, F., S. Nicklen, and A. R. Coulson.** 1977. DNA sequencing with chain-terminating inhibitors. Proc. Natl. Acad. Sci. USA **74:**5463–5467.
29. **Shumilin, I. A., R. H. Kretsinger, and R. H. Bauerle.** 1999. Crystal structure of phenylalanine-regulated 3-deoxy-D-*arabino*-heptulosonate 7-phosphate synthase from *Escherichia coli*. Structure **7:**865–875.
30. **Silakowaki, B., B. Kunze, and R. Müller.** 2000. *Stigmatella aurantiaca* Sg al5 carries genes encoding type I and type II 3-deoxy-D-*arabino*-heptulosonate 7-phosphate synthases: involvement of a type II synthase in aurachin biosynthesis. Arch. Microbiol. **173:**403–411.
31. **Silhavy, T. J., M. L. Berman, and L. W. Enquist (ed.).** 1984. Experiments with gene fusions. Cold Spring Harbor Laboratory, Cold Spring Harbor, N.Y.
32. **Subramaniam, P. S., G. Xie, T. Xia, and R. A. Jensen.** 1998. Substrate ambiguity of 3-deoxy-D-*manno*-octulosonate 8-phosphate synthase from *Neisseria gonorrhoeae* in the context of its membership in a protein family containing a subset of 3-deoxy-D-*arabino*-heptulosonate 7-phosphate synthases. J. Bacteriol. **180:**119–127.
33. **Van Wageningen, A., P. Kirkpatrick, D. Williams, B. Harris, J. Kershaw, N. Lennard, M. Jones, S. Jones, and P. Solenberg.** 1998. Sequencing and analysis of genes involved in the biosynthesis of a vancomycin group antibiotic. Chem. Biol. **3:**155–162.
34. **Walker, G. E., B. Dunbar, I. S. Hunter, H. G. Nimmo, and J. R. Coggins.** 1996. Evidence for a novel class of microbial 3-deoxy-D-arabino-heptulosonate-7-phosphate synthases in *Streptomyces coelicolor* A3(2), *Streptomyces rimosus* and *Neurospora crassa*. Microbiology **142:**1973–1982.
35. **Wallace, B. J., and J. Pittard.** 1967. Genetic and biochemical analysis of the isoenzymes concerned in the first reaction of aromatic biosynthesis in *Escherichia coli*. J. Bacteriol. **93:**234–244.
36. **Whitaker, R. J., A. Berry, G. S. Byng, M. J. Fiske, and R. A. Jensen.** 1985. Clues from *Xanthomonas campestris* about the evolution of aromatic biosynthesis and its regulation. J. Mol. Evol. **21:**139–149.